

1 Title: Finite element analysis of air gun impact on post-keratoplasty eye

2

3 Name of authors: Kanno Okamura, Asami Shimokawa, Rie Takahashi, Yusuke Saeki,

4 Hiroaki Ozaki, Eiichi Uchio

5

6 Affiliations of authors: Department of Ophthalmology, Fukuoka University School of

7 Medicine, Fukuoka, Japan

8

9 Abstract

10

11 Purpose: Due to the mechanical vulnerability of eyes that have undergone penetrating  
12 keratoplasty (PKP), it is clinically important to evaluate the possibility of corneal wound  
13 dehiscence by blunt impact. We have previously developed a simulation model  
14 resembling a human eye based on information obtained from cadaver eyes and applied  
15 three-dimensional finite element analysis (FEA) to determine the physical and  
16 mechanical response to an air gun impact at various velocities on the post-PKP eye.

17 Methods: Simulations in a human eye model were performed with a computer using a  
18 FEA program created by Nihon, ESI Group. The air gun pellet was set to impact the eye  
19 at three different velocities in straight or 12° up-gaze positions with the addition of  
20 variation in keratoplasty suture strength of 30%, 50% and 100% of normal corneal  
21 strength.

22 Results: Furthermore to little damage in the case of 100% strength, in cases of lower  
23 strength in a straight-gaze position, wound rupture seemed to occur in the early phase  
24 (0.04 – 0.06 ms) of impact at low velocities, while regional break was observed at 0.14  
25 ms after an impact at high velocity (75 m/s). In contrast, wound damage was observed in  
26 the lower quadrant of the suture zone and sclera in 12° up-gaze cases. Wound damage

27 was observed 0.08 ms after an impact threatening corneoscleral laceration, and the  
28 involved area being larger in middle impact velocity (60 m/s) simulations than in lower  
29 impact velocity simulations, and larger damaged area was observed in high impact  
30 velocity cases and leading to corneoscleral laceration.

31 Conclusions: These results suggest that the eye is most susceptible to corneal damage  
32 around the suture area especially with a straight-gaze impact by an air gun, and that  
33 special precautionary measures should be considered in patients who undergo PKP. FEA  
34 using a human eyeball model might be a useful method to analyze and predict the  
35 mechanical features of eyes that undergo keratoplasty.

36 Key Words

37 air gun; finite element analysis; cornea; rupture; keratoplasty

38

39 Running header: Finite element analysis of air gun impact on post-PKP eye

40

41 Corresponding author: Eiichi Uchio, MD, PhD, Department of Ophthalmology, Fukuoka

42 University School of Medicine, 7-45-1 Nanakuma, Jonan-ku, Fukuoka 814-0180, Japan,

43 Phone: +81 92 801 1011, Fax +81 92 865 4445, E-mail: [euchio@fukuoka-u.ac.jp](mailto:euchio@fukuoka-u.ac.jp)

44 Introduction

45

46 Globe rupture in eyes treated by corneal transplantation is a serious clinical condition that  
47 may result in loss of vision.<sup>1-2</sup> Several studies have reported the clinical outcome,  
48 incidence and causes of trauma in cases of globe rupture after keratoplasty.<sup>1-10</sup> The  
49 incidence of traumatic globe dehiscence after penetrating keratoplasty (PKP) has been  
50 reported to be 0.23% - 5.8%.<sup>3,5,8-10</sup> Keratoplasty exposes patients to a higher risk of globe  
51 rupture because the surgical wound may never regain the strength and stability of an intact  
52 cornea [1]. The major types of trauma causing globe rupture in the post-PKP eye are:  
53 being accidentally struck by an object (33%) or child (13%), intentional trauma (20%)  
54 and falls (13%) [3]. In other studies, major causes of globe rupture in eyes undergoing  
55 keratoplasty were falls in elderly patients followed by blunt trauma, from a branch, airbag,  
56 fist or finger.<sup>1,5</sup> Due to the mechanical vulnerability of eyes that undergo keratoplasty, it  
57 is clinically important to evaluate the corneal wound strength against blunt impact, and  
58 the risk of traumatic wound dehiscence. However, it is difficult to evaluate strain strength  
59 property of the post-keratoplasty eye, because an apparatus for measuring mechanical  
60 features of the eye has not been developed or introduced in clinical ophthalmology, and  
61 the possibility of tissue damage by these tests cannot be excluded, especially in a clinical

62 situation.

63 A recent study reported increased damage with increased pressure and a shift in the  
64 damage profile over time in a mouse model of primary ocular blast injury using a device  
65 consisting of a pressurized air tank attached to a regulated paintball gun with a machined  
66 barrel.<sup>11</sup> However, this study did not evaluate open ocular injury caused by blast injury.<sup>11</sup>

67 Therefore, we planned to research the kinetic phenomenon of blunt trauma to eyes that  
68 have undergone keratoplasty in a simulation method. Creating a human-like eye with raw  
69 data from the human eye for biomechanical simulations using finite element analysis  
70 (FEA) would help to investigate and better explain the physical and physiological  
71 responses to impact injuries.<sup>12</sup> The other important benefit of biomechanical analysis  
72 obtained with computer models is that they may reduce the need for animal studies over  
73 time, which being increasingly restricted on ethical grounds.

74 We have previously developed a simulation model resembling a human eye based on  
75 information obtained from cadaver eyes, and applied three-dimensional FEA to determine  
76 the physical and mechanical conditions of impacting foreign bodies that cause an  
77 intraocular foreign body.<sup>13</sup> This model of the human eye was also used in our studies on  
78 airbag impact in the post-radial keratotomy eye,<sup>14</sup> post-transsclerally fixated posterior  
79 chamber intraocular lens (PC-IOL) eye,<sup>15</sup> and after photorefractive keratectomy.<sup>16</sup> After

80 refinement of the FEA model, we have recently evaluated the threshold of impact velocity  
81 of an air bag to induce suture breakage or globe rupture in the post-transsclerally fixated  
82 PC-IOL eye with different axial lengths, by using FEA.<sup>17</sup>

83 It was reported that the mean time from corneal keratoplasty to globe rupture or wound  
84 dehiscence was 6.5 months – 6.2 years.<sup>1-3,7-8</sup> Except for the report by Rohrbach et al,<sup>2</sup> the  
85 interval between keratoplasty and traumatic wound dehiscence ranged from 6.5 to 22  
86 months in other studies.<sup>1,7-8</sup> It is interesting that corneal wound dehiscence occurred most  
87 frequently (37%) within the first year after surgery,<sup>3</sup> and 37.5% of traumatic ruptures  
88 occurred in the first postoperative month.<sup>9</sup> These reports suggest that the occurrence of  
89 corneal wound rupture depends on wound strength after surgery, and visual disability  
90 early after surgery also increases the risk of blunt trauma. Collating these factors, in this  
91 study, we extended the simulation model after revision to further determine the physical  
92 and mechanical response to an air gun impact at various velocities on the post-  
93 keratoplasty eye, with consideration of recovery of wound strength in a stepwise range  
94 using FEA.

95

96 Materials and methods

97

98 A model human eye was created and used in computer simulations performed with FEA

99 program, PAM-GENERIS™ (Nihon ESI, Tokyo, Japan), described elsewhere.<sup>13</sup> The

100 model eye was created by setting the mass density of the cornea and sclera as constants,

101 and element types including the three layers of the model eye (outer, middle and inner)

102 as variables for meshing principles (Figure 1-A).<sup>13</sup> The material properties and geometry

103 of the model were obtained from past experiments with three pairs of human cadaver

104 eyes.<sup>13</sup> The elastic properties and meshing principles of the model human eye were similar

105 to those in previous reports.<sup>13-14</sup> Poisson ratios of the cornea at 0.420 kg/mm<sup>3</sup> and the

106 sclera at 0.470 kg/mm<sup>3</sup> were used to determine the standard stress strain curves for the

107 cornea and sclera.<sup>18-20</sup> The cornea was assumed to be spherical, with a central thickness

108 of 0.5 mm and a central radius of curvature of 7.8 mm. The anterior chamber was set at a

109 depth of 5.1 mm. The vitreous length was assumed to be 18.6 mm, and the posterior

110 curvature of the retina was assumed to be 12.0 mm. The mass densities of ocular tissues

111 from past reports were applied as follows: cornea, 1.149 kg/mm<sup>3</sup>; sclera, 1.243 kg/mm<sup>3</sup>;

112 vitreous humor, 1.002 kg/mm<sup>3</sup> and aqueous humor, 1.000 kg/mm<sup>3</sup>. A vitreous model as a

113 solid mass was also assigned with a hydrostatic pressure of 20 mmHg (2.7 kPa).



114 A biomechanical head of a dummy was created, assuming that everything excluding the  
115 eye was a solid element, to reduce the computing time. The Hybrid III model was  
116 modified by replacing the head of the dummy with a biomechanical model of the head in  
117 which an eye with a transplanted corneal graft was inserted.<sup>18,21</sup> An air gun pellet (0.2 g),  
118 with 6 mm diameter and higher rigidity than an eyeball, was set to impact the eyeball in  
119 a straight- or 12° up-gaze position (Figure 1-B) at initial velocities of 45, 60 and 75 m/s.  
120 The reference point for globe rupture was then calculated to be at a strain of 18.0% and  
121 stress of 9.45 MPa for the cornea, and at a strain of 6.8% and stress of 9.49 MPa for the  
122 sclera, which exceeded the tensile tolerance based on element deletion method.<sup>14</sup> A new  
123 approach in this study was the addition of variation of keratoplasty suture strength of 30%,  
124 50% and 100% of normal corneal strength, instead of calculating the limit of tensile force  
125 (N) of a 10-0 nylon suture. The suture region was assigned between 5.5 mm and 7.5 mm  
126 diameter, and strain that exceeded the tensile tolerance in this region was set to 5.4%,  
127 9.0% and 18.0% in the case of strength variation of 30%, 50% and 100%, respectively.  
128 Changes in the deformity of the eye and the strain induced were calculated by Virtual  
129 Performance Solver (VPS) (Nihon ESI) and evaluated by color mapping (Figure 1-C).  
130 Breakage of the corneal suture was defined as the point at which the strain becomes  
131 intolerable due to deformation of the eye caused by air gun impact, when the strain

132 exceeds the strain or stress value of the cornea based on element deletion method.<sup>22</sup> In  
133 this study, the mapping properties were also revised owing to the development of  
134 computer technology since the previous study.<sup>17</sup> Corneal wound strain was recorded  
135 sequentially at all velocities, and deformation of the eye was displayed sequentially in  
136 milliseconds in slow motion.  
137

138 Results

139

140 Abundant data were extracted from this simulation study. Thus, it is difficult to display  
141 all the results. The results of each condition are shown in the frontal view, side view and  
142 sectional view of the deformed globe. Maximum strain observed in the frontal view was  
143 also obtained in all simulation conditions. Due to two eye gaze positions ( $0^\circ$  and  $12^\circ$ ),  
144 three strength variations (30%, 50% and 100%), and three impact velocities of the air gun  
145 (45, 60 and 75 m/s), 18 cases were simulated sequentially from the primary impact to the  
146 eyeball until 0.2 ms after the primary impact. Figure 2 shows the sequential change of  
147 maximum strain displayed graphically with color in 18 simulation conditions. Figure 2-  
148 A shows the result of a case of  $0^\circ$  gaze, 30% strength and 45 m/s impact velocity (0-30-  
149 45), for example.

150 In general, simulation showed corneal damage was observed in all cases in the straight-  
151 gaze position (Table 1). However, the extent of damage varied according to the situation.  
152 In cases of 100% strength of the sutured region in the straight-gaze position, corneal strain  
153 hardly reached its threshold and graft dehiscence was not expected to occur in simulation  
154 (Figure 2-G (0-100-45), Figure 2-H (0-100-60) and Figure 2-I (0-100-75)). In cases of  
155 50% strength in the straight-gaze position, wound rupture seemed to occur in the early

156 phase (0.04 – 0.06 ms) of impact at low speeds in simulation (Figure 2-D (0-50-45),  
157 Figure 2-E (0-50-60)). Despite the high impact velocity (75 m/s), simulation showed  
158 corneal strain was limited in the early phase, but regional break was observed at 0.14 ms  
159 after the impact (Figure 2-F (0-50-75)). Similar results were observed in cases of 30%  
160 strength in the straight-gaze position, and the corneal damage was dependent on the  
161 impact velocity (Figure 2-A (0-30-45) and Figure 2-B (0-30-60)), while regional break  
162 was found in the late phase (0.14 ms after impact) in cases with an impact velocity of 75  
163 m/s in simulation (Figure 2-C (0-30-75)).

164 In contrast, simulation showed wound damage was observed in the lower quadrant of the  
165 cornea and adjacent sclera in 12° up-gaze cases (Table 1). Wound laceration hardly  
166 occurred at low impact velocity (45 m/s) (Figure 2-M (12-50-45) and Figure 2-P (12-30-  
167 45)) even in cases of 30% strength in simulation (Figure 2-J (12-100-45)). At middle  
168 impact velocity (60 m/s), simulation showed wound damage was observed at 0.08 ms  
169 after the impact threatening corneoscleral laceration (Figure 2-K (12-30-60), Figure 2-N  
170 (12-50-60) and Figure 2-Q (12-100-60)), and its area was larger than that in cases with  
171 low impact velocity. A larger damaged area was observed in high impact velocity cases  
172 and corneoscleral laceration was inevitable, while the extent of the damage did not show  
173 an apparent difference among all strengths in simulation (Figure 2-L (12-30-75), Figure

174 2-O (12-50-75) and Figure 2-R (12-100-75)).

175 Discussion

176

177 Unlike with human bones and the ribcage, the injury biomechanics of soft organs, such  
178 as the human eye, are difficult to simulate due to limited available mechanical information.

179 In addition, it is hard to simulate common causes of blunt trauma, such as from a finger,  
180 corner of a hard object or floor, because it is hard to estimate the physiological properties

181 and impact velocity of these situations for simulation study. Thus, we selected an air gun  
182 pellet as the impacting object on the post-keratoplasty eye in this study because the

183 physical properties and penetration speed are well known. While air gun ocular injury is  
184 a frequent cause of blunt trauma in children,<sup>23-27</sup> blunt ocular rupture in the post-

185 keratoplasty eye occurs relatively often in elderly patients.<sup>5</sup> The incidence of globe  
186 rupture was reported to be 2.0% in eyes receiving PKP and 0.5% in eyes receiving deep

187 anterior lamellar keratoplasty (DALK).<sup>5</sup> The reported incidence of traumatic graft  
188 dehiscence among PKP eyes was 2.3 per 1000 person-years, and few cases of graft

189 dehiscence were observed after DALK in other studies.<sup>6,14</sup> These studies indicate that  
190 globe rupture after keratoplasty is a rare complication, and the incidence was higher after

191 PKP than after DALK. Therefore, we carried out a simulation study on eyes after PKP in  
192 this study. However, it should be noted that globe rupture might occur in cases of DALK,<sup>6</sup>

193 and Descemet's membrane might be considered a barrier against possible trauma, but  
194 there have been reports of cases of globe rupture after radial keratotomy<sup>28</sup> and laser in  
195 situ keratomileusis.<sup>29</sup> The cause of the dislocation of corneal graft was a fall or blunt  
196 trauma, from a branch, airbag, fist, or finger, in other reports.<sup>4-5</sup> An air gun shot to the eye,  
197 especially to the post-keratoplasty eye, is a rare accident, but it can mimic an impact with  
198 a small object such as a branch, finger or fist; thus, this situation was adopted in this study.  
199 However, from the clinical standpoint in real life, a more common impacting object, such  
200 as an airbag while driving, seems more suitable for a simulation study of ocular injury,  
201 and we are planning a further simulation study based on our simulation model.

202 In this study, different results were observed in the two gaze positions. In straight-gaze  
203 position simulations, the avoidance of corneal laceration in 100% strength cases means  
204 that air gun impact does not necessarily result in serious globe damage if the property of  
205 the cornea is intact; in contrast, the damaged area coincided with the suture area and  
206 wound laceration was observed in the early phase (0.04 – 0.06 ms after the impact) in  
207 30% and 50% strength cases at impact velocities of 45 m/s and 60 m/s, while regional  
208 break was observed at the same strength at high impact velocity (75 m/s) in the late phase  
209 (0.14 ms after the impact). The reason for the discordance in the phase of wound  
210 dehiscence between low - middle impact velocities and high impact velocity is unclear;

211 however, these phenomena suggest the possibility of differences in kinetic and  
212 mechanical behavior after air gun impact according to the impact velocity on a  
213 millisecond scale, meaning that these so-called microenvironmental movements cannot  
214 be visualized unless a simulation study is carried out. Regarding postsurgical wound  
215 strength in PKP, several studies have been reported. Histopathological studies confirm  
216 that corneal wounds never regain their original strength, meaning that wound weakness  
217 persists for a long period after keratoplasty.<sup>30-31</sup> Histopathological changes including  
218 incarceration of Bowman's or Descemet's membrane or retrocorneal fibrous tissue sealing  
219 the wound have been observed 25 years after surgery, indicating that corneal wounds  
220 continue to remain weak.<sup>30</sup> Furthermore, postmortem studies of eyes that underwent PKP  
221 show incomplete wound healing microscopically at the graft-donor interface in 86.7% of  
222 patients.<sup>31</sup> The results of these studies suggest that corneal damage around the suture area  
223 is most susceptible, especially in a straight-gaze impact by an air gun, and support our  
224 results.

225 In the simulation of 12° up-gaze, except at low impact velocity, corneoscleral damage and  
226 possible laceration were observed at middle and high impact velocities. The reason for  
227 these different results compared with straight-gaze simulations was not clear; however,  
228 the correlation between impact velocity and severity of the damaged area was considered



229 to derive from the speculation that scleral factors play a more critical role in eccentric air  
230 gun impact due to kinetic energy also concentrated on the eccentric globe surface. We  
231 selected the 12° up-gaze position as the representation of a closing eye; therefore, these  
232 results support that prompt eye closing including protection of the eyelid itself may avoid  
233 serious corneal suture damage after PKP. Combining these results with those of our  
234 present study, it can be proposed that special precautionary measures should be  
235 considered in patients who have undergone PKP, especially elderly persons who are prone  
236 to injuries such as falls and being hit by objects. Therefore, detailed advice from  
237 ophthalmologists to avoid serious trauma including protective eyewear such as goggles  
238 is essential for patients who undergo PKP, even a long time after surgery. Recent studies  
239 also report that serious pediatric corneal damage has been increasing by air guns meaning  
240 that ocular damage is easily occur in 100% strength (intact) eye.<sup>32-33</sup> These studies  
241 indicate the increasing necessity of regulations for eye protection, sales, and usage of air  
242 guns to prevent juvenile ocular injury due to air guns.<sup>32-33</sup>

243 There are several limitations of this study. First, weakness of the graft-recipient junction  
244 was simulated as a regional strain limit decrease in this study, while wound dehiscence  
245 occurs linearly around the graft-recipient junction clinically even if the suture remains  
246 across the graft-recipient junction. However, it is impossible to simulate a linear, so-called

247 single dimensional, strength decrease in the current simulation model; therefore, we  
248 introduced a concentric, so-called two-dimensional, sutured region in this study. Further  
249 refinement in computer technology will enable us to carry out more accurate simulation  
250 of air gun ocular impact that is closer to the clinical situation. Secondly, in several  
251 simulation cases, especially those with high impact velocity in the straight-gaze position,  
252 graphic output terminated before 0.16 ms. Because a high velocity air gun pellet has a  
253 tendency to move into the eyeball due to its high energy, further simulation was  
254 interrupted according to element deletion method.<sup>14</sup> These results, on the other hand,  
255 reflect the possibility of an intraocular foreign body injury from an air gun pellet as a  
256 small object penetrating injury.

257 In conclusion, FEA using a human eyeball model might be a useful method to analyze  
258 and predict the mechanical features of blunt ocular trauma after surgery including  
259 keratoplasty. The present study also revealed that wound suture strength, which has a  
260 critical relation with wound healing, primarily affects the clinical outcome and visual  
261 prognosis of blunt trauma such as that due to an air gun impact.

262 Disclosure

263 The authors report no conflict of interest in this work.

264

265 Ethics

266 The tissue from human cadavers referred to in this study relates to earlier, entirely separate

267 experiments, and that no human tissue was used specifically for the study.

268

269 Acknowledgements

270

271 This work was supported by a Grant-in-Aid for Encouragement of Scientists (15K10911)

272 from the Ministry of Education, Science, Sports and Culture of Japan. We thank Dr. W.

273 Gray for editing this manuscript. This is a post-peer-review, pre-copyedit version of an

274 article published in *Clinical Ophthalmology*. The final authenticated version is available

275 online at: <https://doi.org/10.2147/OPTH.S236825>.

276

277 References

278

279 1. Tzelikis PF, Fenelon EM, Yoshimoto RR, Rascop GP, Queiroz RL, Hida WT. Traumatic  
280 wound dehiscence after corneal keratoplasty. *Arq Bras Oftalmol.* 2015;78(5): 310-312.

281 2. Rohrbach JM, Weidle EG, Steuhl KP, Meilinger S, Pleyer U. Traumatic wound  
282 dehiscence after penetrating keratoplasty. *Acta Ophthalmol Scand.* 1996;74(5):501-505.

283 3. Meyer JJ, McGhee CN. Incidence, severity and outcomes of traumatic wound  
284 dehiscence following penetrating and deep anterior lamellar keratoplasty. *Br J*  
285 *Ophthalmol.* 2016;100(10):1412-1415.

286 4. Steinberg J, Eddy MT, Katz T, Fricke OH, Richard G, Linke SJ. Traumatic wound  
287 dehiscence after penetrating keratoplasty: case series and literature review. *Eur J*  
288 *Ophthalmol.* 2012;22(3):335-341.

289 5. Kawashima M, Kawakita T, Shimmura S, Tsubota K, Shimazaki J. Characteristics of  
290 traumatic globe rupture after keratoplasty. *Ophthalmology.* 2009;116(11):2072-2076.

291 6. Kalantan H, Al-Shahwan S, Al-Torbak A. Traumatic globe rupture after deep anterior  
292 lamellar keratoplasty. *Indian J Ophthalmol.* 2007;55(1):69-70.

293 7. Agrawal V, Wagh M, Krishnamachary M, Rao GN, Gupta S. Traumatic wound  
294 dehiscence after penetrating keratoplasty. *Cornea.* 1995;14(6):601-603.

- 295 8. Bowman RJ1, Yorston D, Aitchison TC, McIntyre B, Kirkness CM. Traumatic wound  
296 rupture after penetrating keratoplasty in Africa. *Br J Ophthalmol*. 1999;83(5):530-534.
- 297 9. Elder MJ, Stack RR. Globe rupture following penetrating keratoplasty: how often, why,  
298 and what can we do to prevent it? *Cornea*. 2004;23(8):776-780.
- 299 10. Lam FC, Rahman MQ, Ramaesh K. Traumatic wound dehiscence after penetrating  
300 keratoplasty-a cause for concern. *Eye (Lond)*. 2007;21(9):1146-1150.
- 301 11. Hines-Beard J, Marchetta J, Gordon S, Chaum E, Geisert EE, Rex TS. A mouse model  
302 of ocular blast injury that induces closed globe anterior and posterior pole damage. *Exp*  
303 *Eye Res*. 2012;99(3):63-70.
- 304 12. Viano DC, King AI, Melvin JW, Weber K. Injury biomechanics research: an essential  
305 element in the prevention of trauma. *J Biomech*. 1989;2(5):403-417.
- 306 13. Uchio E, Ohno S, Kudoh J, Aoki K, Kisielwicz LT. Simulation model of an eyeball  
307 based on finite element analysis method on a supercomputer. *Br J Ophthalmol*.  
308 1999;3(10):1106-1111.
- 309 14. Uchio E, Ohno S, Kudoh K, Kadosono K, Andoh K, Kisielwicz LT. Simulation of  
310 airbag impact on post-radial keratotomy eye using finite element analysis. *J Cataract*  
311 *Refract Surg*. 2001;27(11):1847-1853.
- 312 15. Uchio E, Watanabe Y, Kadosono K, Matsuoka Y, Goto S. Simulation of airbag

313 impact on eyes with transsclerally fixated posterior chamber intraocular lens using finite  
314 element analysis. *J Cataract Refract Surg.* 2004;30(2):483-490.

315 16. Uchio E, Kadonosono K, Matsuoka Y, Goto S. Simulation of airbag impact on eyes  
316 after photorefractive keratectomy by finite element analysis method. *Graefes Arch Clin*  
317 *Exp Ophthalmol.* 2003;241(6):497-504.

318 17. Huang J, Uchio E, Goto S. Simulation of airbag impact on eyes with different axial  
319 lengths after transsclerally fixated posterior chamber intraocular lens by using finite  
320 element analysis. *Clin Ophthalmol.* 2015;9:263-270.

321 18. Buzard KA. Introduction to biomechanics of the cornea. *Refract Corneal Surg.*  
322 1992;8(2):127-138.

323 19. Greene PR. Closed-form ametropic pressure-volume and ocular rigidity solutions. *Am*  
324 *J Optom Physiol Opt.* 1985;62(12):870-878.

325 20. Hoeltzel DA, Altman P, Buzard K, Choe K. Strip extensimetry for comparison of the  
326 mechanical response of bovine, rabbit, and human corneas. *J Biomech Eng.*  
327 1992;114(2):202-215.

328 21. Ruan JS, Prasad P. Coupling of a finite element human head model with a lumped  
329 parameter Hybrid III dummy model: preliminary results. *J Neurotrauma.*  
330 1995;12(4):725-734.

- 331 22. Jiang B, Zhu F, Cao L, Presley BR, Shen MS, Yang KH. Computational study of  
332 fracture characteristics in infant skulls using a simplified finite element model. *J Forensic*  
333 *Sci.* 2017;62(1):39-49.
- 334 23. Shuttleworth GN, Galloway P, Sparrow JM, Lane C. Ocular air gun injuries: a one-  
335 year surveillance study in the UK and Eire (BOSU). 2001-2002. *Eye (Lond).* 2009;  
336 23(6):1370-1376.
- 337 24. Shuttleworth GN, Galloway PH. Ocular air-gun injury: 19 cases. *J R Soc Med.*  
338 2001;94(8):396-399.
- 339 25. Aziz M, Patel S. BB gun-related open globe injuries. *Ophthalmol Retina.*  
340 2018;2(10):1056-1061.
- 341 26. Ahmadabadi MN, Karkhaneh R, Valeshabad AK, Tabatabai A, Jager MJ, Ahmadabadi  
342 EN. Clinical presentation and outcome of perforating ocular injuries due to BB guns: a  
343 case series. *Injury.* 2011;42(5):492-495.
- 344 27. Ramstead C, Ng M, Rudnisky CJ. Ocular injuries associated with airsoft guns: a case  
345 series. *Can J Ophthalmol.* 2008;43(5):584-587.
- 346 28. Rashid ER, Waring GO 3rd. Complications of radial and transverse keratotomy. *Surv*  
347 *Ophthalmol.* 1989;34(2):73-106.
- 348 29. Sun CC, Chang SW, Tsai RR. Traumatic corneal perforation with epithelial ingrowth



- 349 after laser in situ keratomileusis. *Arch Ophthalmol.* 2001;119(6):907-909.
- 350 30. Flaxel JT, Swan KC. Limbal wound healing after cataract extraction. A histologic  
351 study. *Arch Ophthalmol.* 1969;81(5):653-659.
- 352 31. Lang GK, Green WR, Maumenee AE. Clinicopathologic studies of keratoplasty eyes  
353 obtained post mortem. *Am J Ophthalmol.* 1986;101(1):28-40.
- 354 32. Lee R, Fredrick D. Pediatric eye injuries due to nonpowder guns in the United States,  
355 2002-2012. *J AAPOS.* 2015;19(2):163-168.
- 356 33. Jovanović MB. Eye injuries caused by shotgun and air-rifles treated at the University  
357 Eye Clinic in Belgrade 2000-2009. *Srp Arh Celok Lek.* 2014;142(1-2):6-9.

358 Legends for figures

359

360 Figure 1. Simulation profile of model eye and deformation scale

361 (A) Sagittal and diagonal views of model eye and meshing principles of finite element  
362 analysis. (B) Eyeball and impacting air gun location in straight- (left) and 12° up-gaze  
363 (right) positions. (C) Color mapping scale of deformation of eye showing strain induced;  
364 warmer color of red represents greater deformation. Strain strength that induces corneal  
365 laceration is simulated to occur at 18.0% (red) and scleral laceration is simulated to occur  
366 at 6.8% (blue green).

367

368 Figure 2. Sequential deformation of post-penetrating keratoplasty model eye upon airsoft

369 gun impact at three different velocities and three different strain strengths in sutured area.

370 (A) Case of straight-gaze position, strain strength 30% and impact velocity 45 m/s (0-30-  
371 45). (B) Case of straight-gaze position, strain strength 30% and impact velocity 60 m/s  
372 (0-30-60). (C) Case of straight-gaze position, strain strength 30% and impact velocity 75  
373 m/s (0-30-75). (D) Case of straight-gaze position, strain strength 50% and impact velocity  
374 45 m/s (0-50-45). (E) Case of straight-gaze position, strain strength 50% and impact  
375 velocity 60 m/s (0-50-60). (F) Case of straight-gaze position, strain strength 50% and

376 impact velocity 75 m/s (0-50-75). (G) Case of straight-gaze position, strain strength 100%  
377 and impact velocity 45 m/s (0-100-45). (H) Case of straight-gaze position, strain strength  
378 100% and impact velocity 60 m/s (0-100-60). (I) Case of straight-gaze position, strain  
379 strength 100% and impact velocity 75 m/s (0-100-75). (J) Case of 12° up-gaze position,  
380 strain strength 30% and impact velocity 45 m/s (12-30-45). (K) Case of 12° up-gaze  
381 position, strain strength 30% and impact velocity 60 m/s (12-30-60). (L) Case of 12° up-  
382 gaze position, strain strength 30% and impact velocity 75 m/s (12-30-75). (M) Case of  
383 12° up-gaze position, strain strength 50% and impact velocity 45 m/s (12-50-45). (N)  
384 Case of 12° up-gaze position, strain strength 50% and impact velocity 60 m/s (12-50-60).  
385 (O) Case of 12° up-gaze position, strain strength 50% and impact velocity 75 m/s (12-50-  
386 75). (P) Case of 12° up-gaze position, strain strength 100% and impact velocity 45 m/s  
387 (12-100-45). (Q) Case of 12° up-gaze position, strain strength 100% and impact velocity  
388 60 m/s (12-100-60). (R) Case of 12° up-gaze position, strain strength 100% and impact  
389 velocity 75 m/s (12-100-75).

390 Table 1. Summary of ocular damage observed in simulation

391

---

Straight gaze position			
Strength of the suture area (%)	100%	50%	30%
Impact velocity (m/s)			
45	graft intact	wound rupture	wound rupture
60	graft intact	wound rupture	wound rupture
75	graft intact	regional break	regional break

---

12° up-gaze position			
Strength of the suture area (%)	100%	50%	30%
Impact velocity (m/s)			

---

---

45	graft intact	graft intact	graft intact
60	corneoscleral laceration	corneoscleral laceration	corneoscleral laceration
75	corneoscleral laceration	corneoscleral laceration	corneoscleral laceration

---

392

393

394

395

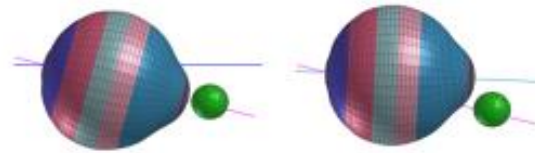
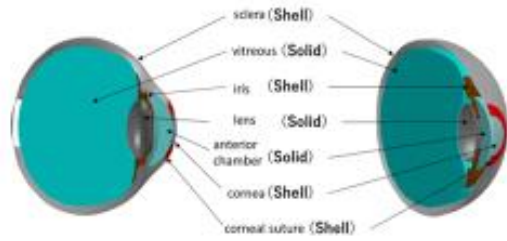
396

397

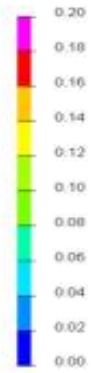
398

399

400



A

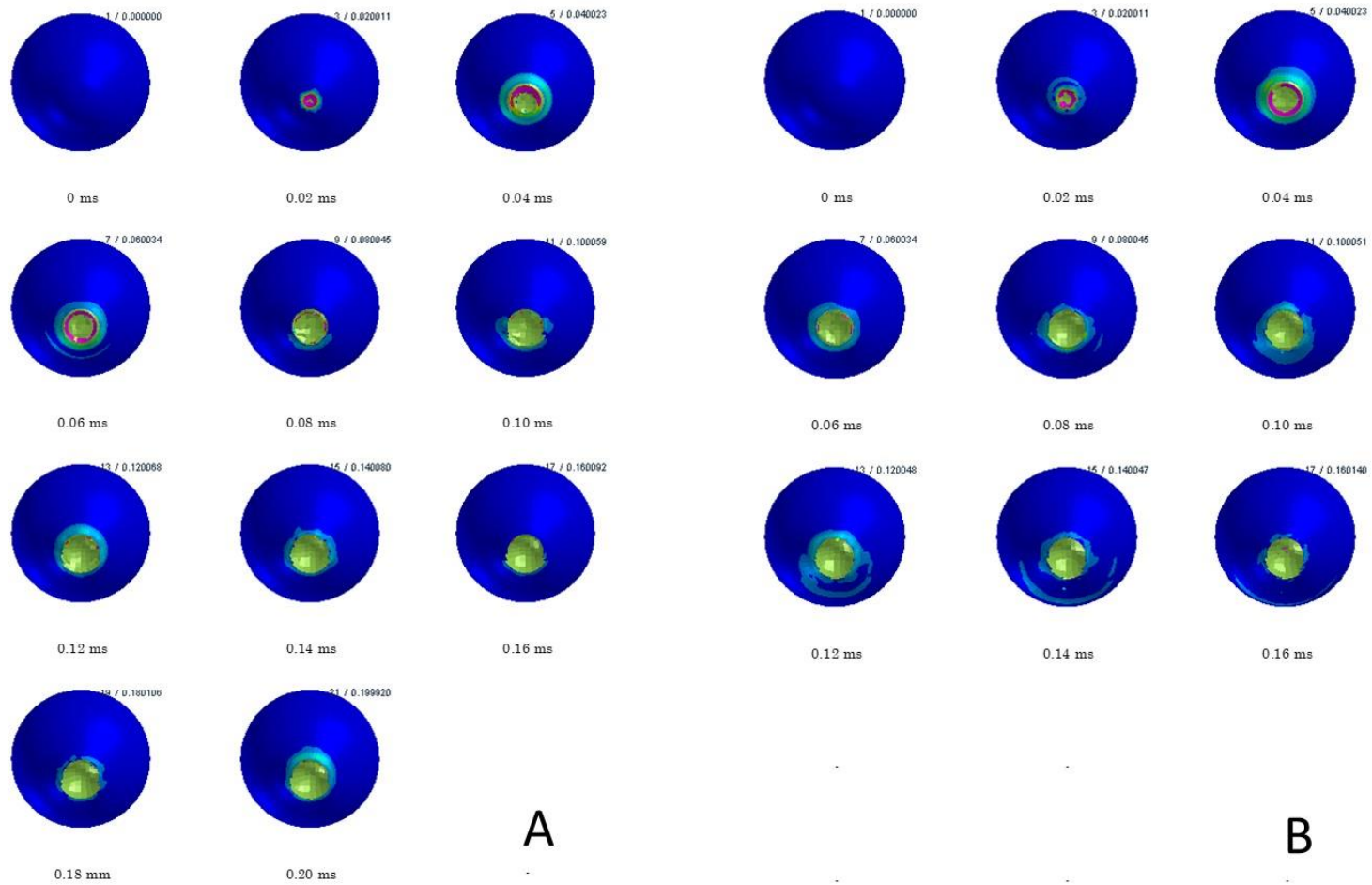


C

Figure 1

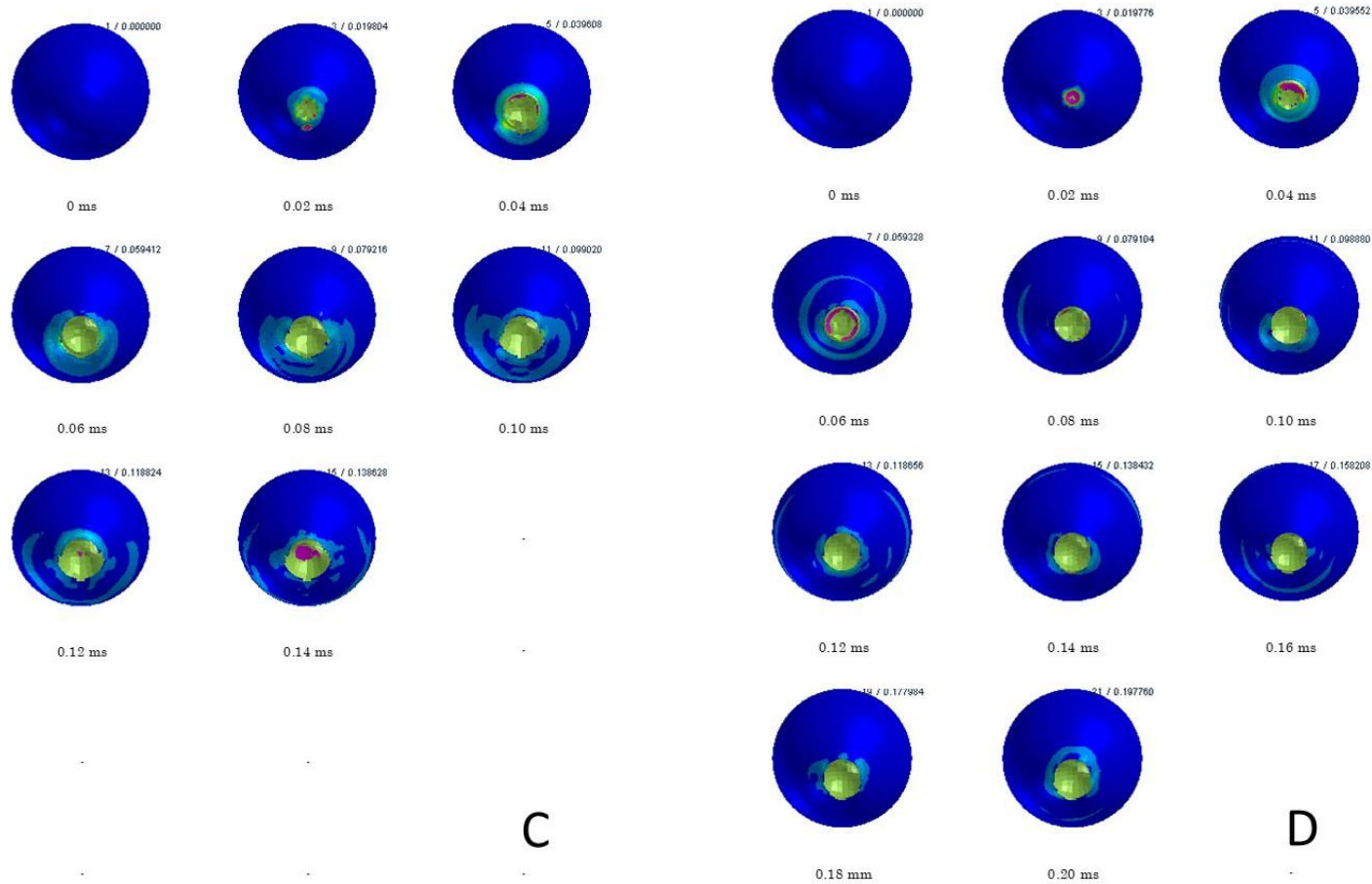
401

402



403

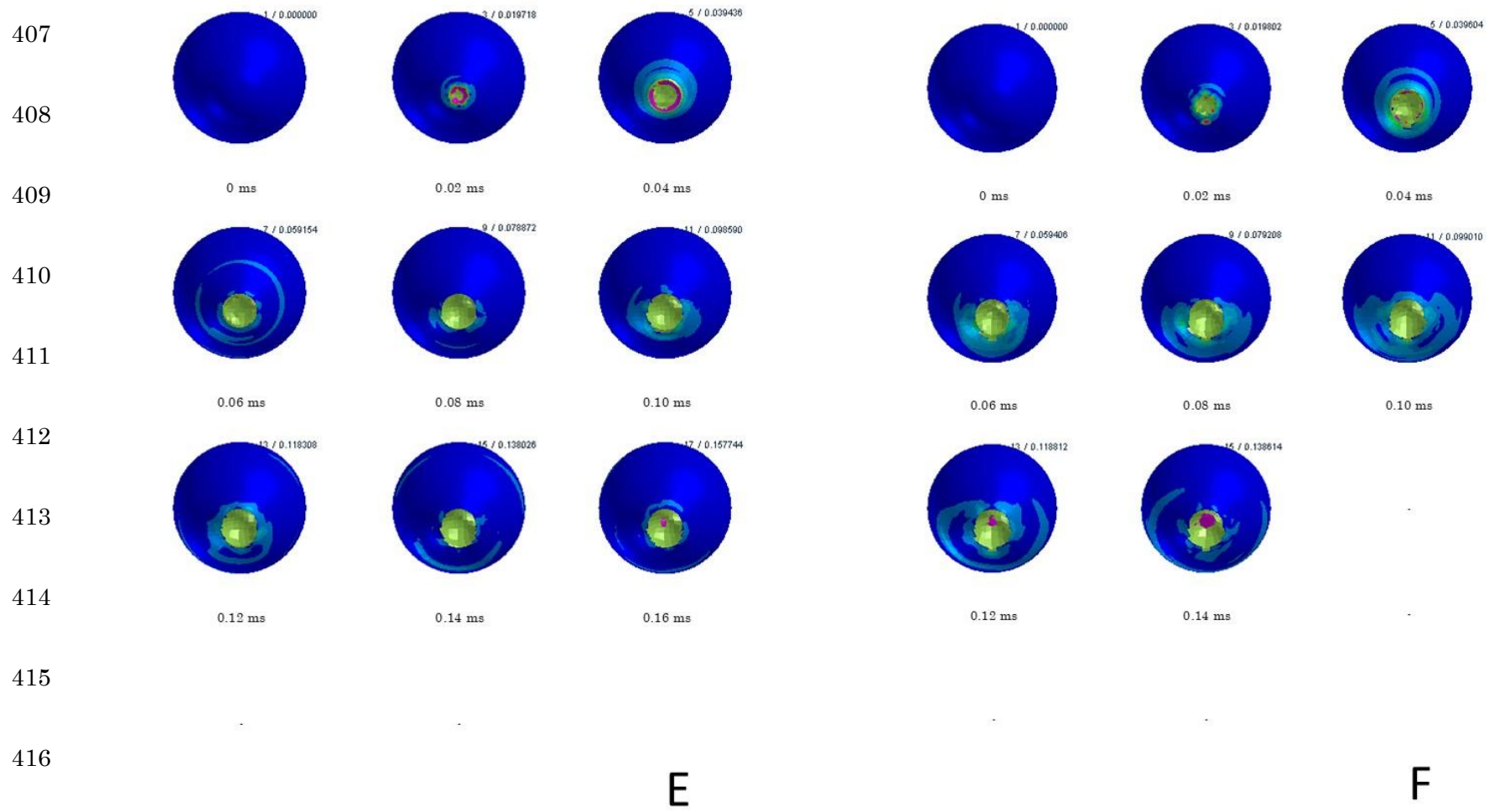
404 Figure 2



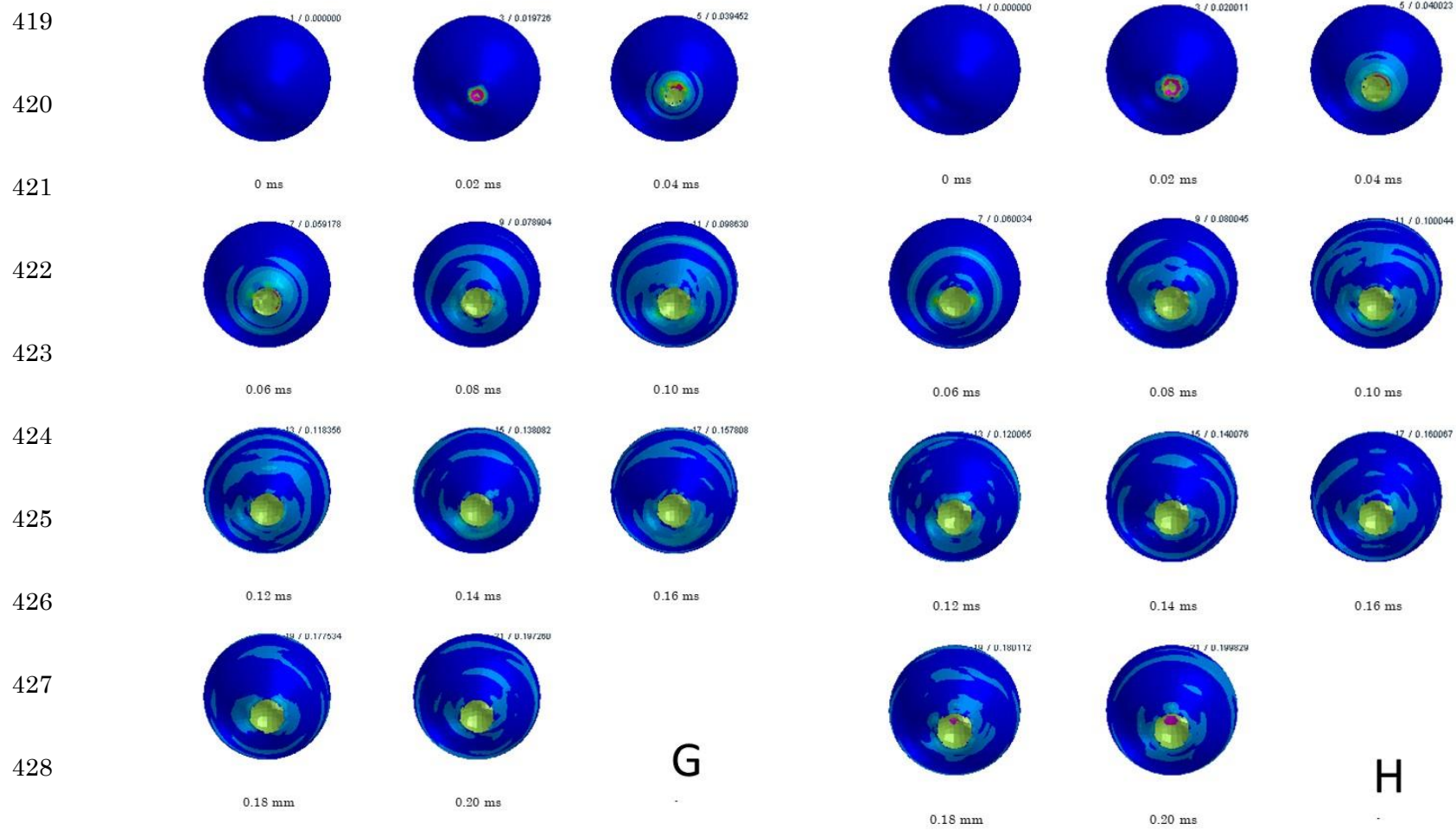
405

406 Figure 2-continued

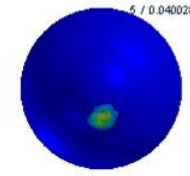
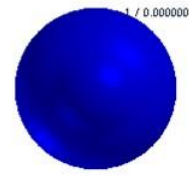
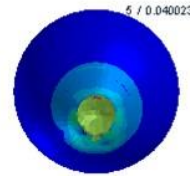
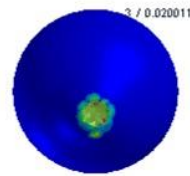
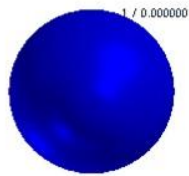




418 Figure 2-continued



431



432

433

0 ms

0.02 ms

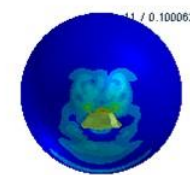
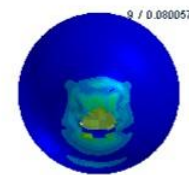
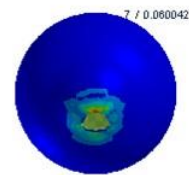
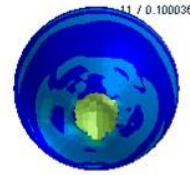
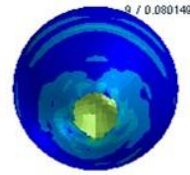
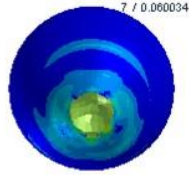
0.04 ms

0 ms

0.02 ms

0.04 ms

434



435

436

0.06 ms

0.08 ms

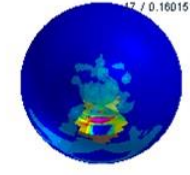
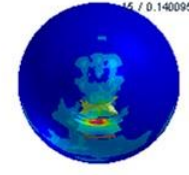
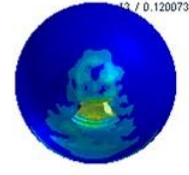
0.10 ms

0.06 ms

0.08 ms

0.10 ms

437



438

0.12 ms

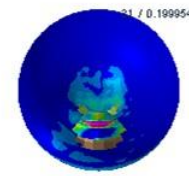
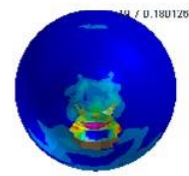
0.12 ms

0.14 ms

0.16 ms

439

440



0.18 ms

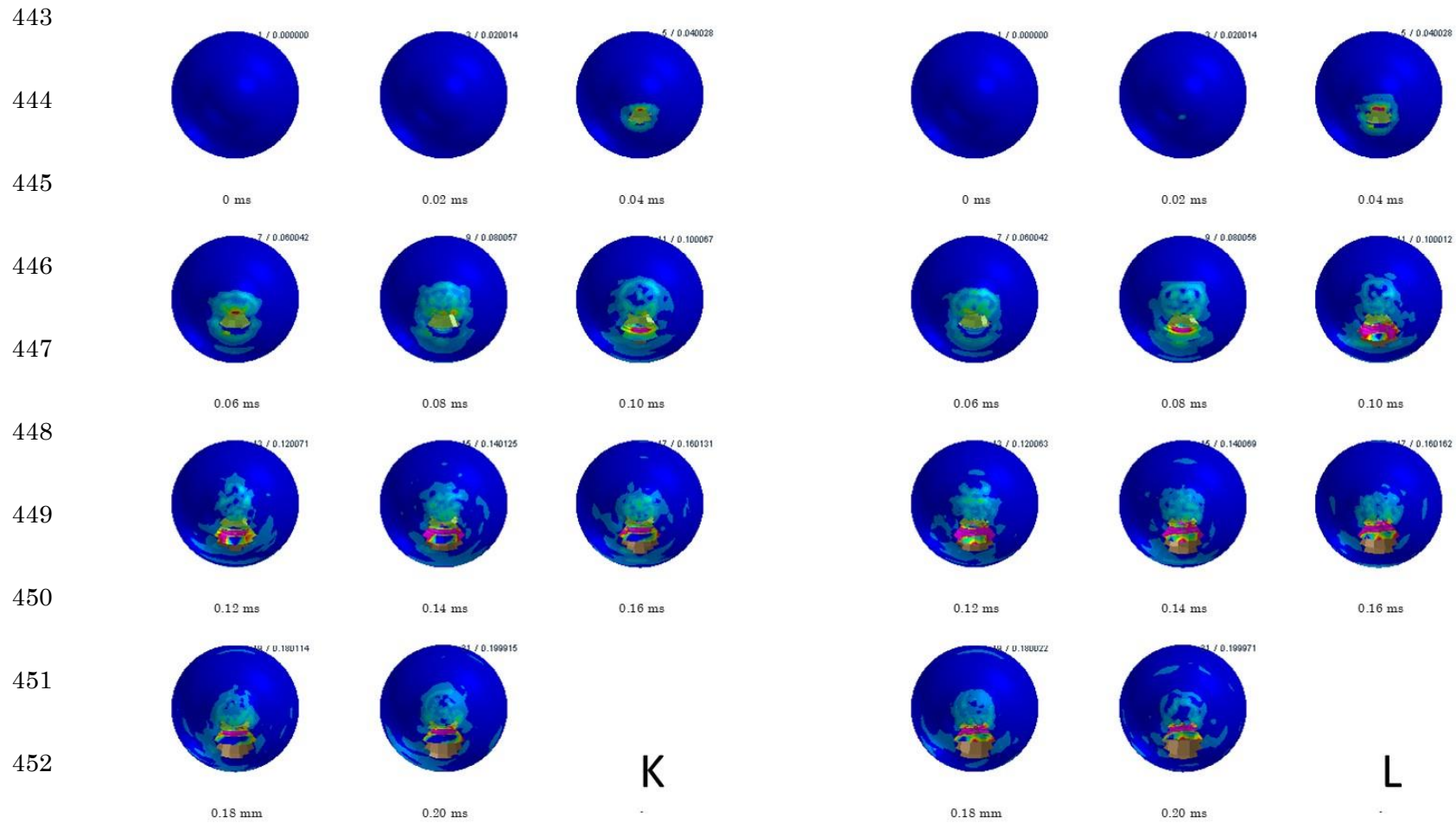
0.20 ms

441

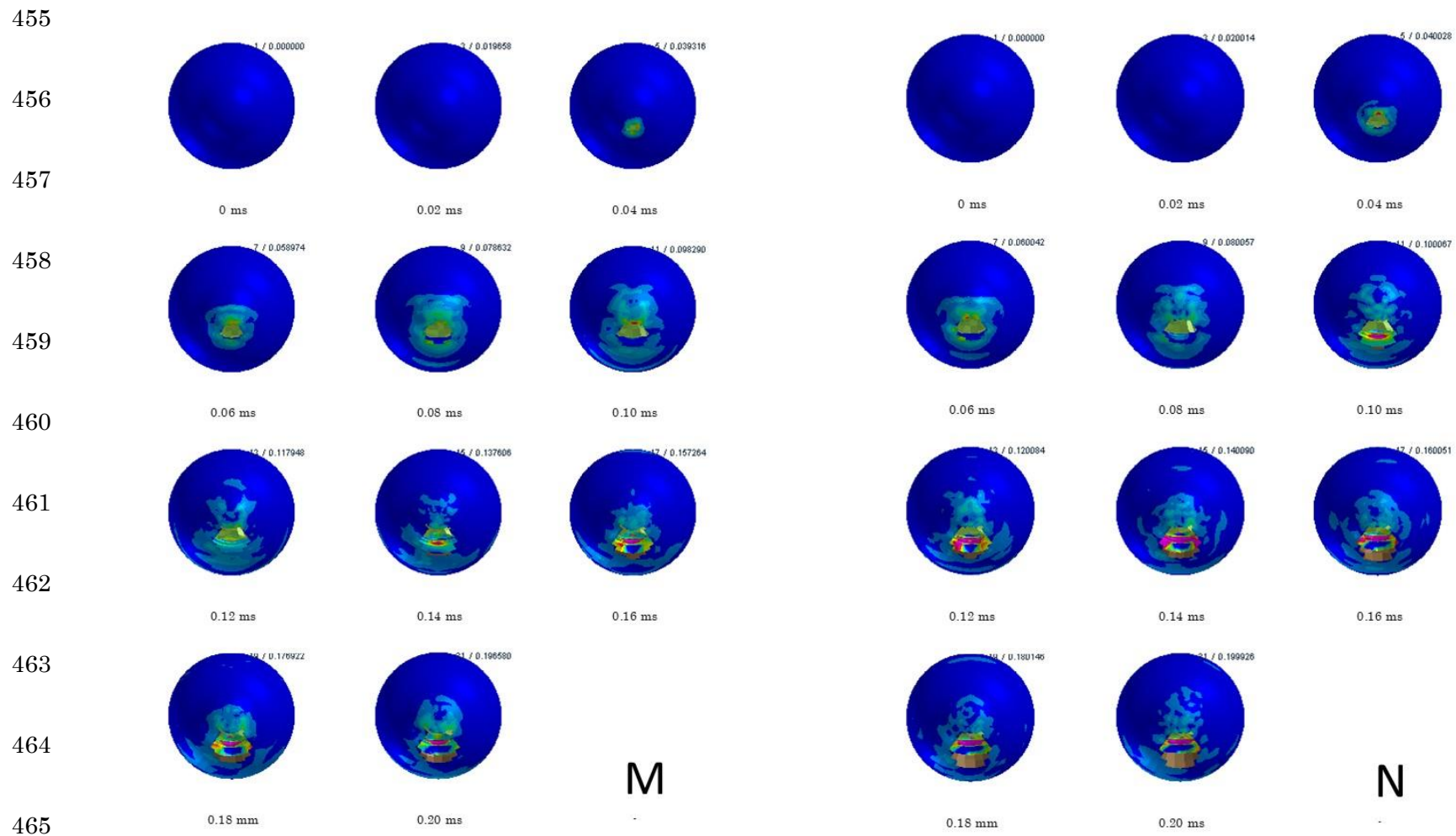
I

J

442 Figure 2-continued

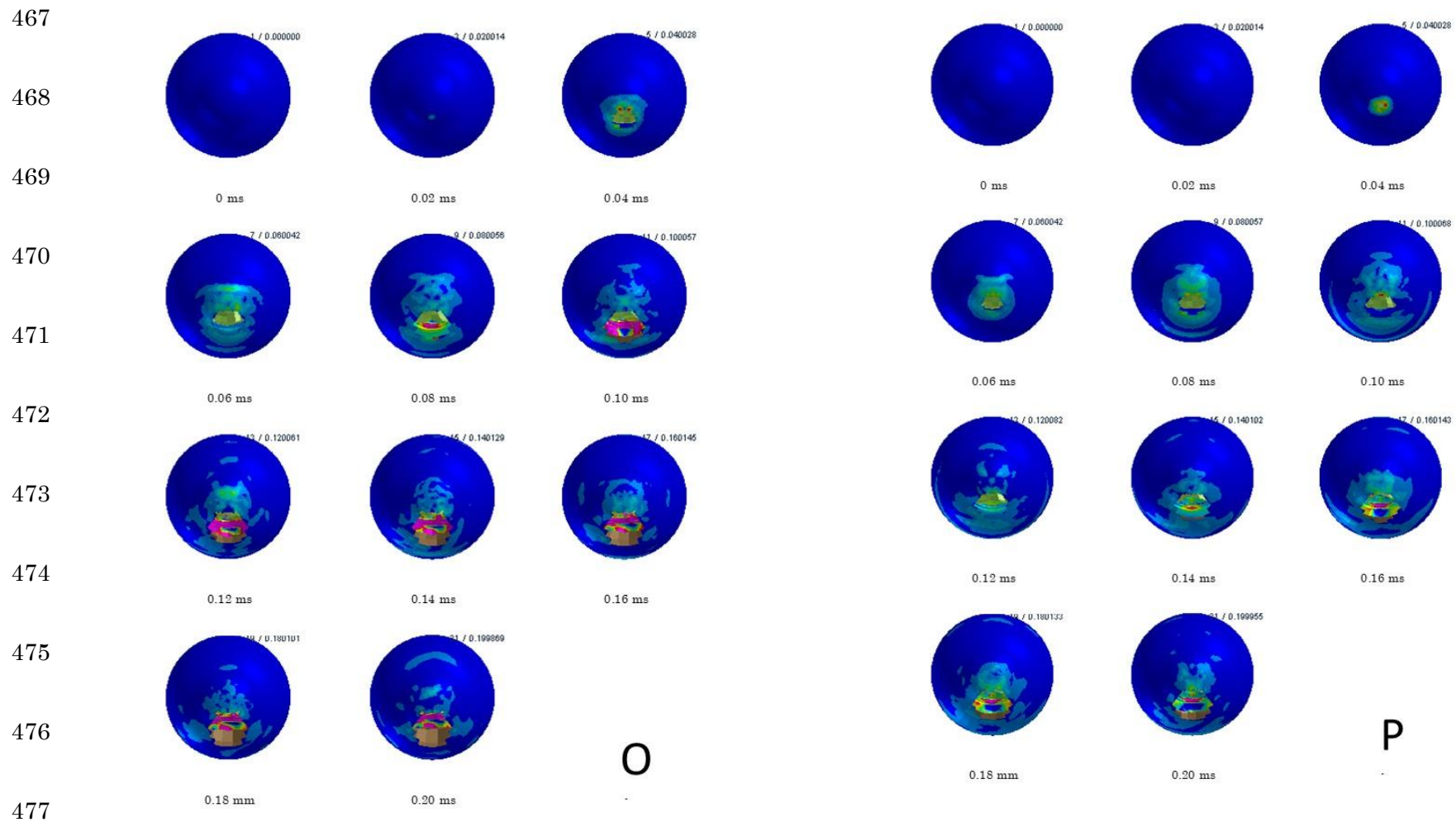


454 Figure 2-continued

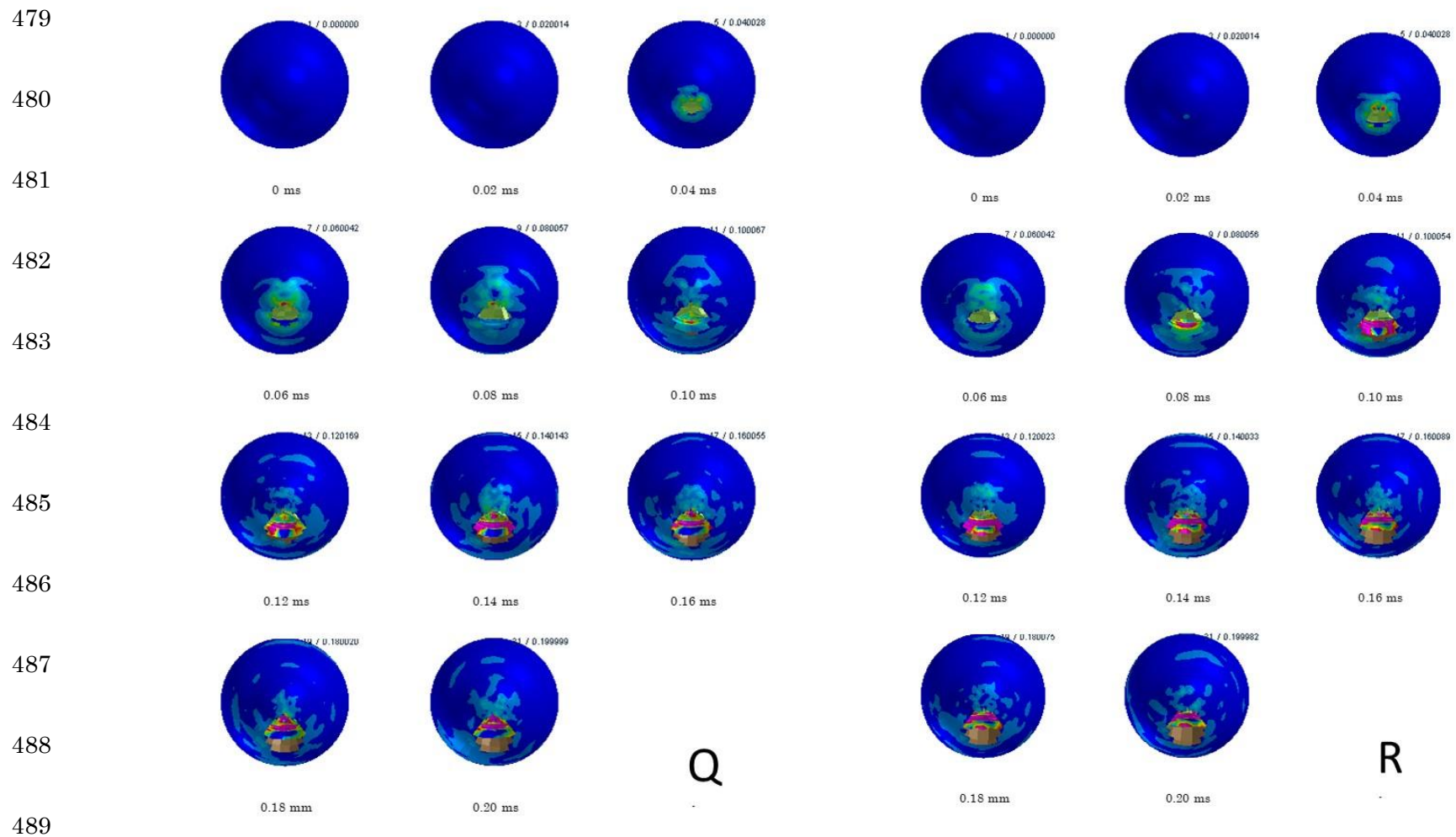


466 Figure 2-continued





478 Figure 2-continued



490 Figure 2-continued